

# Viscosity and Speed of Sound of Potassium Nitrate and Lithium Nitrate in Poly(ethylene glycol)

Gautam Kalita,<sup>†</sup> Krishna G. Sarma,<sup>‡</sup> and Sekh Mahiuddin<sup>\*,†</sup>

Material Science Division, Regional Research Laboratory, Jorhat-785006, Assam, India, and  
Department of Chemistry, Dibrugarh University, Dibrugarh-786004, Assam, India

Densities, viscosities, and speeds of sound of  $0.15[x\text{KNO}_3 + (1 - x)\text{LiNO}_3] + 0.85[\text{poly}(\text{ethylene glycol})]$  and  $0.20[x\text{KNO}_3 + (1 - x)\text{LiNO}_3] + 0.80[\text{poly}(\text{ethylene glycol})]$  systems (molecular weight of poly(ethylene glycol) = 300) were measured as functions of composition ( $x = 0.0$  to  $1.0$  mole fraction) and temperature ( $273.15 \leq T/K \leq 343.15$ ). The viscosity and the structural relaxation time were found to be non-Arrhenius temperature dependent and were analyzed by using the Vogel–Tamman–Fulcher equation. The normalized viscosity isotherm exhibits a significant mixed alkali effect for the  $0.20[x\text{KNO}_3 + (1 - x)\text{LiNO}_3] + 0.80[\text{poly}(\text{ethylene glycol})]$  system at  $273.15$  K. The onset of the mixed alkali effect in this system has been explained by the competitive polarization model. The absence of the mixed alkali effect in the  $0.15[x\text{KNO}_3 + (1 - x)\text{LiNO}_3] + 0.85[\text{poly}(\text{ethylene glycol})]$  system is attributed to the lesser amount of total alkali ion content in the system.

## Introduction

Studies on the mixed alkali effect<sup>1–5</sup> (MAE) and its phenomenological influence on the isotherms of dynamic properties (electrical conductivity, viscosity, and diffusion) as functions of composition and temperature in molecular liquid media<sup>6,7</sup> are limited. Recently, the MAE has been investigated using a mixed alkali cation pair in poly(ethylene oxide) and poly(propylene oxide), which differ from low molar mass solvent systems in the mechanism of cation transport.<sup>8,9</sup> A few systems of mixed alkali cation pairs have shown the MAE as a maxima in the conductivity isotherms,<sup>10</sup> whereas some other systems have exhibited a negative deviation from the additivity in the electrical conductivity isotherms.<sup>11</sup> On the other hand, Teeters and Norton<sup>12</sup> have failed to detect the MAE in poly(propylene oxide)–Na/KSCN systems at all in the conductivity isotherms. A minimum in the conductivity isotherms has been reported by Teeters and Hill<sup>8</sup> in poly(ethylene oxide)–Na/KSCN systems while no deviation in the conductivity isotherms was observed in poly(propylene oxide)–Na/KSCN systems.

The onset of the MAE was discussed in terms of the relaxation time of the local structure of the polymer matrix and the ion diffusion. On the other hand, we have demonstrated that even if the deviation in the viscosity and the conductivity isotherms is found to be a few percent (viz.,  $\sim 1.5\%$ ), the normalized viscosity and conductivity isotherms, as proposed by Easteal,<sup>3</sup> exhibit a significant MAE of manyfold (viz.,  $\sim 44\%$ ).<sup>5</sup> In systems containing mixed alkali cation pairs in polymers, the MAE has been investigated by measuring the electrical conductivity. In general, electrical conductivity, viscosity, and diffusion are used to detect the MAE in ternary systems containing a mixed alkali cation pair. We, therefore, in this communication,

report viscosities and speeds of sound of  $0.15[x\text{KNO}_3 + (1 - x)\text{LiNO}_3] + 0.85[\text{poly}(\text{ethylene glycol})]$  and  $0.20[x\text{KNO}_3 + (1 - x)\text{LiNO}_3] + 0.80[\text{poly}(\text{ethylene glycol})]$  systems as functions of temperature and composition to investigate the existence of the MAE.

## Experimental Section

Both  $\text{KNO}_3$  ( $>99\%$ , E. Merck, India) and  $\text{LiNO}_3$  ( $>98\%$ , E. Merck, India) were recrystallized twice from triple-distilled water and dried over  $\text{P}_2\text{O}_5$  in a vacuum desiccator. Poly(ethylene glycol) of formula weight 300 (henceforth PEG300) ( $>99\%$ , E. Merck, India) was used as solvent without further purification. Depending on the solubility of  $\text{KNO}_3$  and  $\text{LiNO}_3$  in PEG300, we have selected  $0.15[x\text{KNO}_3 + (1 - x)\text{LiNO}_3] + 0.85[\text{PEG300}]$  and  $0.20[x\text{KNO}_3 + (1 - x)\text{LiNO}_3] + 0.80[\text{PEG300}]$  systems, where  $x$  is the mole fraction. All solutions were prepared by mass.

A single-stem graduated pycnometer was used to measure densities. The reproducibility of the densities of an individual sample was within  $\pm 0.1\%$ . Viscosity measurements were made with the help of a Schott Geräte AVS310 unit using Ubbelohde viscometers having the cell constants  $0.3127 \text{ mm}^2 \cdot \text{s}^{-2}$  and  $0.9895 \text{ mm}^2 \cdot \text{s}^{-2}$ , respectively. The reproducibility between the duplicate viscosities of an individual sample was found to be within  $\pm 0.4\%$ . Speeds of sound in all solutions were measured with an accuracy of  $\pm 0.1 \text{ m} \cdot \text{s}^{-1}$  by using a multifrequency ultrasonic interferometer M-18 (Mittal Enterprises, India).

All measurements were made as functions of composition ( $x = 0.0$  to  $1.0$  mol fraction) and temperature ( $273.15 \leq T/K \leq 343.15$ ). A thermostat type Schott Geräte-CT1450, a Lauda-RLS6D, or a Julabo-F32 was used, depending on the temperature range, to maintain the temperature of the study to  $\pm 0.02$  K.

## Results and Discussion

The measured densities,  $\rho$ , for both the systems have been presented in Table 1 and are found to be a linear function of temperature at a fixed composition (Table 2).

\* To whom all correspondence should be addressed. Fax: 0091-376-370011. E-mail: mahirrjlt@yahoo.com.

<sup>†</sup> Regional Research Laboratory.

<sup>‡</sup> Dibrugarh University.

**Table 1. Densities,  $\rho$ , of 0.15[xKNO<sub>3</sub> + (1 - x)LiNO<sub>3</sub>] + 0.85[PEG300] and 0.20[xKNO<sub>3</sub> + (1 - x)LiNO<sub>3</sub>] + 0.80[PEG300] Systems as Functions of Temperature and Composition**

<i>T</i> /K	$\rho$ /kg·m <sup>-3</sup>	<i>T</i> /K	$\rho$ /kg·m <sup>-3</sup>	<i>T</i> /K	$\rho$ /kg·m <sup>-3</sup>
0.15[xKNO <sub>3</sub> + (1-x)LiNO <sub>3</sub> ] + 0.85 [PEG300]					
<i>x</i> = 0.0		<i>x</i> = 0.2		<i>x</i> = 0.4	
310.95	1139.7	305.55	1145.9	312.55	1141.9
312.90	1138.1	307.50	1144.3	314.55	1139.7
314.80	1136.4	309.50	1142.1	316.55	1138.3
317.00	1134.3	311.60	1140.7	318.55	1136.7
319.00	1132.8	313.45	1139.1	320.65	1135.1
320.95	1131.3	315.50	1137.6	322.50	1133.6
323.00	1129.7	317.40	1136.0	324.50	1132.2
324.80	1128.2	319.45	1134.6	326.45	1130.9
326.75	1126.8	321.35	1133.3	328.20	1129.5
328.70	1125.5	323.10	1131.9	330.25	1128.0
330.55	1124.2	325.20	1130.4	332.05	1126.5
332.45	1122.6	327.05	1128.9		
		329.10	1126.9		
		330.95	1125.4		
<i>x</i> = 0.6		<i>x</i> = 0.8		<i>x</i> = 1.0	
311.45	1144.8	307.70	1150.0	310.05	1149.5
313.45	1142.6	309.90	1148.4	311.95	1147.9
315.55	1141.1	311.80	1146.8	314.10	1145.7
317.45	1139.5	313.80	1144.6	316.15	1144.2
319.60	1138.0	316.00	1143.1	318.05	1142.6
321.45	1136.4	317.85	1141.5	320.20	1141.1
323.45	1135.1	319.95	1140.0	322.15	1139.5
325.30	1133.8	321.85	1138.4	324.05	1138.2
327.20	1132.4	323.95	1137.0	326.05	1136.9
329.25	1130.8	325.80	1135.8	327.95	1135.5
331.10	1129.3	327.70	1134.3	329.90	1133.9
333.20	1127.3	329.65	1132.8	331.85	1132.4
		331.60	1131.3		
0.20[xKNO <sub>3</sub> + (1 - x)LiNO <sub>3</sub> ] + 0.80[PEG300]					
<i>x</i> = 0.0		<i>x</i> = 0.2		<i>x</i> = 0.4	
307.35	1152.5	305.80	1156.2	306.10	1158.8
309.25	1150.9	307.85	1154.6	308.20	1157.2
311.35	1149.3	309.90	1153.0	310.30	1155.6
313.40	1147.6	313.90	1149.1	312.40	1154.0
315.35	1145.4	315.95	1147.7	314.45	1152.3
317.40	1144.0	318.00	1146.1	316.55	1150.1
319.45	1142.4	320.10	1144.5	318.70	1148.7
321.50	1140.8	322.00	1142.9	320.55	1147.1
325.15	1137.9	323.95	1141.6	322.45	1145.5
327.35	1136.6	325.95	1140.3	324.75	1143.9
329.15	1135.2	327.80	1138.9	326.75	1142.6
331.15	1133.6	329.90	1137.3	328.75	1141.3
333.10	1132.2	331.80	1135.8	330.60	1139.9
				332.55	1138.3
<i>x</i> = 0.6		<i>x</i> = 0.8		<i>x</i> = 1.0	
306.70	1160.2	304.90	1163.8	309.55	1162.5
308.75	1158.6	306.95	1162.1	311.60	1160.3
311.00	1156.9	309.10	1160.5	313.75	1158.8
313.05	1155.3	311.15	1158.2	315.65	1157.2
315.10	1153.1	313.15	1156.8	317.80	1155.6
317.35	1151.6	315.45	1155.2	319.75	1154.0
319.20	1150.0	317.25	1153.6	321.80	1152.7
321.45	1148.4	319.20	1152.0	323.85	1151.4
323.35	1146.8	321.20	1150.6	325.75	1149.9
325.25	1145.5	323.25	1149.3	327.75	1148.4
327.35	1144.2	325.15	1147.9	329.80	1146.8
329.15	1142.8	327.20	1146.3	331.70	1144.8
331.25	1141.2	329.20	1144.8		
333.15	1139.7	331.10	1142.8		

Viscosities and speeds of sound for both the systems are presented in Tables 3 and 4, respectively. Poly(ethylene glycol) was >90% pure. The dispersity effect of poly(ethylene glycol) on viscosity and speed of sound was not studied.

Viscosities for both the systems showed a non-Arrhenius temperature dependence (~25–28% deviation from the linearity in the Arrhenius plots of  $\ln \eta$  versus  $1/T$ ) and were

**Table 2. Least-Squares Fitted Values of the Parameters of the Density Equation,  $\rho = a - b/(TK - 273.15)$ , for 0.15[xKNO<sub>3</sub> + (1 - x)LiNO<sub>3</sub>] + 0.85[PEG300] and 0.20[xKNO<sub>3</sub> + (1 - x)LiNO<sub>3</sub>] + 0.80[PEG300] Systems**

<i>x</i>	<i>a</i> /kg·m <sup>-3</sup>	<i>b</i> /kg·m <sup>-3</sup> ·K <sup>-1</sup>	std dev in $\rho$
0.15[xKNO <sub>3</sub> + (1 - x)LiNO <sub>3</sub> ] + 0.85[PEG300]			
0.0	1169.2 ± 0.5	0.7890 ± 0.0100	0.23
0.2	1171.1 ± 0.4	0.7867 ± 0.0081	0.23
0.4	1171.6 ± 0.5	0.7668 ± 0.0099	0.20
0.6	1173.9 ± 0.5	0.7723 ± 0.0101	0.22
0.8	1176.7 ± 0.5	0.7796 ± 0.0098	0.26
1.0	1177.5 ± 0.5	0.7697 ± 0.0110	0.24
0.20[xKNO <sub>3</sub> + (1 - x)LiNO <sub>3</sub> ] + 0.80[PEG300]			
0.0	1179.3 ± 0.5	0.7909 ± 0.0098	0.28
0.2	1181.6 ± 0.4	0.7853 ± 0.0092	0.28
0.4	1184.4 ± 0.4	0.7792 ± 0.0092	0.27
0.6	1186.0 ± 0.4	0.7743 ± 0.0082	0.24
0.8	1188.3 ± 0.4	0.7819 ± 0.0090	0.26
1.0	1189.8 ± 0.5	0.7630 ± 0.0082	0.25

**Table 3. Values of Viscosities for 0.15[xKNO<sub>3</sub> + (1 - x)LiNO<sub>3</sub>] + 0.85[PEG300] and 0.20[xKNO<sub>3</sub> + (1 - x)LiNO<sub>3</sub>] + 0.80[PEG300] Systems**

<i>T</i> /K	$\eta$ /mPa·s <i>x</i> = 0.0	$\eta$ /mPa·s <i>x</i> = 0.2	$\eta$ /mPa·s <i>x</i> = 0.4	$\eta$ /mPa·s <i>x</i> = 0.6	$\eta$ /mPa·s <i>x</i> = 0.8	$\eta$ /mPa·s <i>x</i> = 1.0
0.15[xKNO <sub>3</sub> + (1 - x)LiNO <sub>3</sub> ] + 0.85[PEG300]						
343.15	20.52	20.17	18.96	18.74	18.49	17.51
338.15	24.18	23.84	22.29	21.98	21.67	20.53
333.15	28.78	28.13	26.42	26.06	25.68	24.31
328.15	34.65	33.89	31.76	31.28	30.91	29.11
323.15	41.98	41.15	38.67	37.96	37.33	35.27
318.15	51.87	50.71	47.68	49.54	45.97	43.36
313.15	65.00	63.34	59.70	57.98	57.40	54.09
308.15	82.95	81.12	76.18	74.17	72.89	68.70
303.15	109.2	105.8	98.12	96.80	94.41	88.83
298.15	144.4	140.7	130.6	128.6	125.6	117.4
293.15	196.7	191.3	177.7	174.5	170.5	160.1
288.15	276.0	266.9	248.5	243.2	236.9	222.9
283.15	396.9	383.6	356.4	349.0	339.1	323.3
278.15	590.3	570.2	533.3	518.0	502.5	473.8
273.15	915.5	880.5	826.3	799.8	773.0	729.6
0.20[xKNO <sub>3</sub> + (1 - x)LiNO <sub>3</sub> ] + 0.80[PEG300]						
343.15	25.25	24.04	23.35	22.42	20.60	18.80
338.15	29.92	28.50	27.53	26.50	24.35	22.15
333.15	35.79	34.01	32.79	31.44	28.94	26.35
328.15	43.40	41.19	39.73	38.08	34.95	31.79
323.15	53.35	50.49	48.63	46.54	42.68	38.74
318.15	66.50	61.97	60.48	57.77	52.88	47.96
313.15	84.17	79.62	76.39	72.85	66.61	60.34
308.15	108.7	102.6	98.35	93.70	85.64	77.45
303.15	144.3	134.9	129.1	122.7	112.0	101.2
298.15	194.5	183.9	176.3	167.3	150.2	137.0
293.15	268.9	254.2	242.2	230.0	207.0	188.2
288.15	393.6	360.1	343.0	325.5	293.3	266.8
283.15	568.4	527.0	500.6	473.1	428.6	390.0
278.15	844.9	801.2	758.7	717.2	650.5	591.8
273.15	1342.0	1267.0	1213.0	1128.0	1027.0	937.1

least-squares fitted to the Vogel–Tamman–Fulcher (VTF) equation of the following form:

$$\eta = A_{\eta} \exp[B_{\eta}/(T - T_{0\eta})] \quad (1)$$

where  $A_{\eta}$  and  $B_{\eta}$  are the adjustable parameters and  $T_{0\eta}$  is the ideal glass transition temperature. The least-squares fitted values of the  $A_{\eta}$ ,  $B_{\eta}$ , and  $T_{0\eta}$  parameters of eq 1 are listed in Table 5. Figure 1 illustrates the variation of the ideal glass transition temperature,  $T_{0\eta}$ , as a function of  $x$  for both the systems. The plot of  $T_{0\eta}$  versus  $x$  does not exhibit any deviation from the linearity, unlike the case in other mixed alkali systems.<sup>3–5,7</sup>

The existence of an MAE in the present system can be examined by plotting  $\eta$  versus  $x$  (Figure 2) at different

**Table 4.** Values of Speeds of Sound for 0.15[xKNO<sub>3</sub> + (1 - x)LiNO<sub>3</sub>] + 0.85[PEG300] and 0.20[xKNO<sub>3</sub> + (1 - x)LiNO<sub>3</sub>] + 0.80[PEG300] Systems

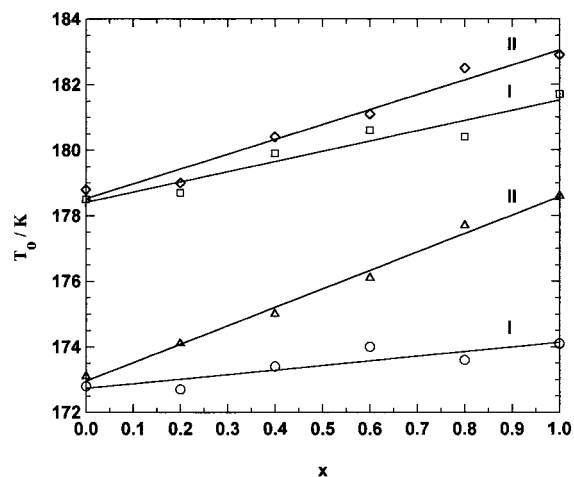
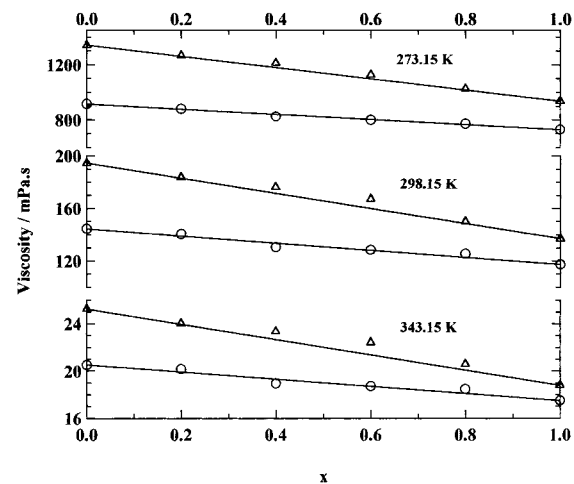
T/K	u/m·s <sup>-1</sup>		u/m·s <sup>-1</sup>		u/m·s <sup>-1</sup>	
	x = 0.0	x = 0.2	x = 0.4	x = 0.6	x = 0.8	x = 1.0
0.15[xKNO <sub>3</sub> + (1 - x)LiNO <sub>3</sub> ] + 0.85[PEG300]						
323.15	1552.3	1550.3	1556.7	1548.4	1543.3	1544.6
318.15	1568.6	1565.2	1571.5	1563.6	1556.1	1562.9
313.15	1584.0	1578.1	1582.6	1577.8	1576.2	1575.0
308.15	1597.7	1594.6	1599.9	1591.7	1587.4	1589.6
303.15	1612.9	1610.7	1616.2	1609.0	1604.5	1609.6
298.15	1628.0	1626.0	1628.5	1624.0	1619.8	1620.5
293.15	1644.8	1641.2	1643.8	1638.6	1633.5	1636.3
288.15	1661.2	1658.6	1660.3	1654.6	1651.0	1653.1
283.15	1675.9	1674.4	1674.2		1667.2	1670.5
278.15	1691.6	1688.0	1688.2	1686.8	1681.9	1687.0
273.15	1709.6	1706.2	1710.0	1709.2	1697.8	1697.3
0.20[xKNO <sub>3</sub> + (1 - x)LiNO <sub>3</sub> ] + 0.80[PEG300]						
323.15	1567.5	1563.7	1561.8	1559.8	1559.9	1563.1
318.15	1582.1	1577.3	1576.7	1573.9	1575.9	1577.0
313.15	1595.4	1591.8	1589.8	1587.2	1588.1	1590.0
308.15	1614.2	1608.6	1605.2	1603.5	1604.0	1605.1
303.15	1626.4	1622.8	1620.2	1619.4	1618.7	1620.5
298.15	1649.1	1636.6	1630.8	1631.5	1633.4	1635.6
293.15	1666.1	1654.3	1652.0	1648.4	1649.4	1647.5
288.15	1678.7	1669.6	1666.7	1663.8	1660.3	1665.6
283.15	1697.3	1681.7	1676.3	1678.2	1678.3	1682.5
278.15	1712.9	1699.5	1695.0	1693.3	1692.8	1696.0
273.15	1729.3	1717.8	1723.7	1710.9	1711.0	1714.6

**Table 5.** Least-Squares Fitted Values of the Parameters of Eq 1 for 0.15[xKNO<sub>3</sub> + (1 - x)LiNO<sub>3</sub>] + 0.85[PEG300] and 0.20[xKNO<sub>3</sub> + (1 - x)LiNO<sub>3</sub>] + 0.80[PEG300] Systems

x	T <sub>0η</sub> /K	A <sub>η</sub> /mPa·s	B <sub>η</sub> /K	std dev in η
0.15[xKNO <sub>3</sub> + (1 - x)LiNO <sub>3</sub> ] + 0.85[PEG300]				
0.0	172.8	0.0876	928.6	0.56
0.2	172.7	0.0882	925.1	0.52
0.4	173.4	0.0869	913.1	1.46
0.6	174.0	0.0919	899.4	0.81
0.8	173.6	0.0902	901.5	0.49
1.0	174.1	0.0877	894.1	1.28
0.20[xKNO <sub>3</sub> + (1 - x)LiNO <sub>3</sub> ] + 0.80[PEG300]				
0.0	173.1	0.0835	969.8	5.48
0.2	174.1	0.0861	950.6	0.98
0.4	175.0	0.0897	933.1	2.07
0.6	176.1	0.0956	910.5	2.02
0.8	177.7	0.0987	883.0	0.75
1.0	178.6	0.0942	870.4	0.70

temperatures. The viscosity isotherms of the 0.15[xKNO<sub>3</sub> + (1 - x)LiNO<sub>3</sub>] + 0.85[PEG300] system (Figure 2) in the temperature range 273.15 K to 343.15 K do not exhibit any deviation from the linearity, whereas the system 0.20[xKNO<sub>3</sub> + (1 - x)LiNO<sub>3</sub>] + 0.80[PEG300] exhibits positive deviations of the order of ~3.0% from the additivity in the viscosity isotherms in the temperature range of the study. The deviations from the additivity are small but more than the uncertainty in the viscosities and may be considered as the onset of the MAE.

The normalized viscosity function,  $F_\eta$ , where  $F_\eta = (\eta_0 - \eta_1)/(\eta_0 - \eta_1)$ ,  $\eta_0$ , and  $\eta_1$  are the viscosities at  $x = 0.0$  and  $x = 1$ , respectively, has been used successfully for comparing viscosity values in different ranges suitably.<sup>3,5</sup> To assess the presence of the MAE, the normalized viscosity isotherms at 273.15 K have been illustrated in Figure 3 as a function of composition. The normalized viscosity isotherm exhibits a significant MAE with ~16.0% deviation from the additivity at  $x = 0.5$  in the 0.20[xKNO<sub>3</sub> + (1 - x)LiNO<sub>3</sub>] + 0.80[PEG300] system (Figure 3). For the 0.15[xKNO<sub>3</sub> + (1 - x)LiNO<sub>3</sub>] + 0.85[PEG300] system, the normalized viscosity isotherm shows a peculiar variation with both positive and negative deviation from the additivity. A similar

**Figure 1.** Variation of ideal glass transition temperature with  $x$  for (I) 0.15[xKNO<sub>3</sub> + (1 - x)LiNO<sub>3</sub>] + 0.85[PEG300] and (II) 0.20[xKNO<sub>3</sub> + (1 - x)LiNO<sub>3</sub>] + 0.80[PEG300] systems: (○, △)  $T_{0\eta}$ ; (◇, □)  $T_{0r}$ . The symbols and the solid lines are observed and calculated values, respectively.**Figure 2.** Plots of viscosity isotherms versus mole fractions,  $x$ , for (○) 0.15[xKNO<sub>3</sub> + (1 - x)LiNO<sub>3</sub>] + 0.85[PEG300] and (△) 0.20[xKNO<sub>3</sub> + (1 - x)LiNO<sub>3</sub>] + 0.80[PEG300] systems. The symbols and the solid lines represent the observed value and the additive properties, respectively.

variation of the normalized viscosity isotherm has also been observed for the 0.3[xKNO<sub>3</sub> + (1 - x)NaNO<sub>3</sub>] + 0.7[Cd(NO<sub>3</sub>)<sub>2</sub>·4H<sub>2</sub>O] melts.<sup>5</sup>

The knowledge of the structural relaxation time,  $\tau$ , is very important for understanding the viscosity behavior with the composition,  $x$ . Therefore, we have calculated the structural relaxation time from the values of the speed of sound (Table 4) using the following relation:<sup>13</sup>

$$\tau = 4\eta\kappa_s/3 = 4\eta/3\rho u^2 \quad (2)$$

where  $\eta$  is the viscosity,  $\kappa_s$  is the isentropic compressibility,  $u$  is the speed of sound, and  $\rho$  is the density of the system.

The dependence of  $\tau$  on temperature is non-Arrhenius in nature (~17 to 19% deviation from the linearity in the Arrhenius plot) and was analyzed by the following VTF type equation:

$$\tau = A_\tau \exp[B_\tau/(T - T_{0\tau})] \quad (3)$$

where  $A_\tau$  and  $B_\tau$  are the adjustable parameters and  $T_{0\tau}$  is the ideal glass transition temperature. The best fit values

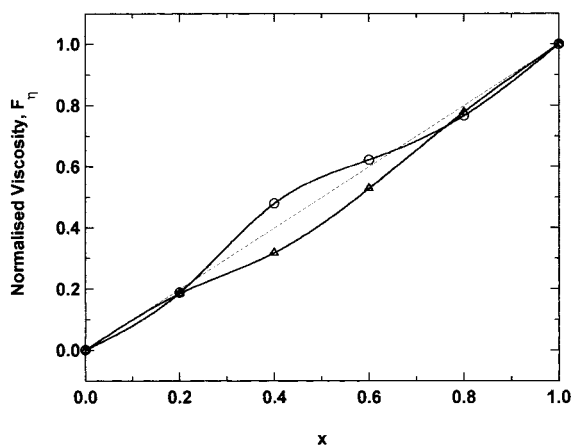


**Figure 3.** Plots of normalized viscosity,  $F_\eta$ , versus  $x$  for (O)  $0.15[x\text{KNO}_3 + (1-x)\text{LiNO}_3] + 0.85[\text{PEG300}]$  and ( $\Delta$ )  $0.20[x\text{KNO}_3 + (1-x)\text{LiNO}_3] + 0.80[\text{PEG300}]$  systems. The symbols and the solid lines represent the observed value and the curve fit, respectively. The broken line represents the additive property.

**Table 6.** Least-Squares Fitted Values of the Parameters of Eq 3 for  $0.15[x\text{KNO}_3 + (1-x)\text{LiNO}_3] + 0.85[\text{PEG300}]$  and  $0.20[x\text{KNO}_3 + (1-x)\text{LiNO}_3] + 0.80[\text{PEG300}]$  Systems

$x$	$T_{0r}/\text{K}$	$A_r/\text{mPa}\cdot\text{s}$	$B_r/\text{K}$	std dev in $\eta$
<b><math>0.15[x\text{KNO}_3 + (1-x)\text{LiNO}_3] + 0.85[\text{PEG300}]</math></b>				
0.0	178.5	0.0091	783.8	0.02
0.2	178.7	0.0093	776.2	0.03
0.4	179.9	0.0092	760.6	0.06
0.6	180.6	0.0104	740.6	0.08
0.8	180.4	0.0099	744.7	0.02
1.0	181.7	0.0099	728.8	0.05
<b><math>0.20[x\text{KNO}_3 + (1-x)\text{LiNO}_3] + 0.80[\text{PEG300}]</math></b>				
0.0	178.8	0.0087	818.9	0.22
0.2	179.0	0.0083	816.8	0.05
0.4	180.4	0.0089	793.6	0.08
0.6	181.1	0.0091	779.6	0.09
0.8	182.5	0.0092	757.8	0.05
1.0	182.9	0.0084	753.7	0.03

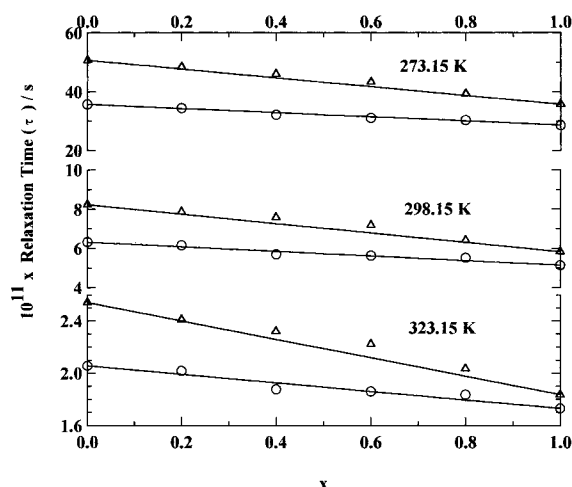


**Figure 4.** Variation of structural relaxation time,  $\tau$ , with mole fraction,  $x$ , for (O)  $0.15[x\text{KNO}_3 + (1-x)\text{LiNO}_3] + 0.85[\text{PEG300}]$  and ( $\Delta$ )  $0.20[x\text{KNO}_3 + (1-x)\text{LiNO}_3] + 0.80[\text{PEG300}]$  systems. The symbols and the solid lines are the observed value and the additive property, respectively.

of the parameters in eq 3 are presented in Table 6. It is apparent that the calculated values of  $T_{0r}$  from eq 3 are reasonably comparable with the  $T_{0\eta}$  obtained from the viscosities for both the systems (Figure 1 and Table 5).

The plots of  $\tau$  versus  $x$  for both the systems at different temperatures are illustrated in Figure 4. From Figure 4 it

is apparent that  $\tau$  decreases as  $\text{Li}^+$  ions are progressively replaced by  $\text{K}^+$  ions for both the systems. The plots of  $\tau$  versus  $x$  isotherms for the  $0.20[x\text{KNO}_3 + (1-x)\text{LiNO}_3] + 0.80[\text{PEG300}]$  system exhibit positive deviations of the order of  $\sim 4\%$  in the temperature range of the study, as also observed in the  $\eta$  versus  $x$  isotherms (Figure 2). The  $0.20[x\text{KNO}_3 + (1-x)\text{LiNO}_3] + 0.80[\text{PEG300}]$  system possesses a higher relaxation time in the  $\text{Li}^+$ -rich region than in the  $\text{K}^+$ -rich region vis-à-vis the viscosity of the systems is higher in the  $\text{Li}^+$ -rich region than in the  $\text{K}^+$ -rich region (Figure 2).

In the present system, the anion  $\text{NO}_3^-$  is attached to the polymer chain through hydrogen bonding with the hydroxyl hydrogen of poly(ethylene glycol). The cation  $\text{Li}^+$  is more polarized toward the  $\text{NO}_3^-$  than the  $\text{K}^+$  due to the smaller ionic radius. As the  $\text{Li}^+$  is progressively replaced by  $\text{K}^+$ , the system becomes less structured, resulting in a decrease in viscosity. In the intermediate composition, when the system contains both  $\text{K}^+$  and  $\text{Li}^+$ , the competitive polarization of the  $\text{NO}_3^-$  toward the  $\text{K}^+$  and  $\text{Li}^+$  produces an unsymmetrical electrical field around the cations. At low temperature, ions and molecules take more time to rearrange themselves in the less available free volume, thereby resulting in a higher relaxation time. This factor along with the competitive polarization of the  $\text{NO}_3^-$  on the  $\text{K}^+$  and  $\text{Li}^+$  contributes to the net positive deviation in the viscosity isotherm in the case of  $0.20[x\text{KNO}_3 + (1-x)\text{LiNO}_3] + 0.80[\text{PEG300}]$  systems. The absence of a detectable MAE in  $0.15[x\text{KNO}_3 + (1-x)\text{LiNO}_3] + 0.85[\text{PEG300}]$  systems may be due to the lesser amount of total alkali ion content in the system.<sup>14</sup>

From the above discussion it is apparent that, in order to exhibit the MAE at a particular temperature, a given system must possess a certain minimum concentration of total alkali ion. At low temperature the system approaches a more rigid structure and thus the cation sites provided by the anion, that is,  $\text{NO}_3^-$  in our present system, become less mobile. Easta<sup>3</sup> suggested that the larger MAE in the network oxide melts in comparison to that of hydrate melts may be due to the difference in mobility of the cation sites; the former have virtually immobile cation sites whereas the anions providing cation sites in the later are relatively mobile. It seems that at 273.15 K, where the system possesses a higher structural relaxation time, the total alkali ion concentration is just sufficient for the onset of the MAE in the  $0.20[x\text{KNO}_3 + (1-x)\text{LiNO}_3] + 0.80[\text{PEG300}]$  systems whereas the  $0.15[x\text{KNO}_3 + (1-x)\text{LiNO}_3] + 0.85[\text{PEG300}]$  system does not possess the critical alkali ion concentration essential for exhibiting the MAE in the temperature range of the study.

#### Acknowledgment

The authors thank the Director of the laboratory and the Head, Material Science Division, for encouragement and interest in this work. One of us (G.K.) is indebted to the Principal and the Head, Department of Chemistry, J. B. College, Jorhat, India, for allowing him to pursue this work.

#### Literature Cited

- Isard, J. O. The Mixed Alkali Effect in Glass. *J. Non-Cryst. Solids* **1969**, *1*, 235–261.
- Day, D. E. Mixed Alkali Glasses-Their Properties and Uses. *J. Non-Cryst. Solids* **1976**, *21*, 343–372.
- Easta, A. J. Equilibrium and transport Properties of  $\text{Ca}(\text{NO}_3)_2 + (\text{Li}, \text{K})\text{NO}_3$  Hydrate Melts: Confirmation of a Mixed Alkali Effect. *Aust. J. Chem.* **1981**, *34*, 1853–1860.

- (4) Sangma, P.; Mahiuddin, S.; Ismail, K. Mixed Alkali Effect in 0.3- $[x\text{KSCN}-(1-x)\text{NaSCN}] - 0.7\text{Ca}(\text{NO}_3)_2 \cdot 4.06\text{H}_2\text{O}$  Melts. *J. Phys. Chem.* **1984**, *88*, 2378–2382.
- (5) Kalita G.; Rohman, N.; Mahiuddin, S. Electrical Conductivity, Viscosity, and Molar Volume of Potassium Nitrate-Sodium Nitrate in Cadmium Nitrate Tetrahydrate Melt. *Aust. J. Chem.* **1998**, *51*, 201–207.
- (6) Gupta, R. L.; Ismail, K. Electrical Conductance of a Mixture of Sodium and Potassium Nitrates in Aqueous Medium. *Can. J. Chem.* **1990**, *68*, 2115–2118.
- (7) Mahiuddin, S. Mixed Alkali Effect in Sodium Thiocyanate-Potassium Thiocyanate-Acetamide Melt Systems. *Can. J. Chem.* **1996**, *74*, 760–765.
- (8) Teeters, D.; Hill, C. M. Comparative Study of the Mixed Alkali Effect in Poly(ethylene oxide) and Poly(propylene oxide)-thiocyanate Salt Systems. *Solid State Ionics* **1994**, *72*, 122–126.
- (9) Perrier, M.; Besner, S.; Paquette, C.; Vallee, A.; Lascaud, S.; Prud'homme, J. Mixed Alkali Effect and Short-Range Interactions in Amorphous Poly(ethylene oxide) Electrolytes. *Electrochim. Acta* **1995**, *40*, 2123–2129.
- (10) Chowdari, B. V. R.; Huq, R.; Farrington, G. C. Thermal and Electrical Characterization of PEO-based Polymer Electrolytes Containing Mixed Cobalt(2) and Lithium(1). *Solid State Ionics* **1992**, *57*, 49–58.
- (11) Teeters, D.; Wong, M.; Straub, C. L. Conductivity and glass transition studies of the mixed alkali effect in poly(propylene oxide)-thiocyanate salt systems. *Solid State Ionics* **1992**, *53/56*, 1083–1086.
- (12) Teeters, D.; Norton, J. C. Mixed Alkali Effect in Poly(propylene oxide)-thiocyanate salt system. *Solid State Ionics* **1991**, *40/41*, 648–650.
- (13) Bender, T. M.; Pecora, R. A Dynamic Light Scattering Study of the *tert*-butyl-Alcohol-Water System. *J. Phys. Chem.* **1986**, *90*, 1770–1706.
- (14) Moynihan, C. T. Mixed Alkali Effect in Hydrate Melts. *J. Electrochem. Soc.* **1979**, *126*, 2144–2149.

Received for review February 7, 2000. Accepted June 15, 2000.

JE0000468